RESEARCH ARTICLE

Molecular
Carcinogenesis WILEY

Antitumor activity of potent pyruvate dehydrogenase kinase 4 inhibitors from plants in pancreatic cancer

Yukihiro Tambe[1] | Tokio Terado[2] | Chul Jang Kim[5] | Ken-ichi Mukaisho[3] | Saori Yoshida[3] | Hiroyuki Sugihara[3] | Hiroyuki Tanaka[4] | Junji Chida[6] | Hiroshi Kido[6] | Kenzaburo Yamaji[7] | Tsuyoshi Yamamoto[7] | Hirofumi Nakano[7,8] | Satoshi Omura[7] | Hirokazu Inoue[1] ⓘ

[1]Division of Microbiology and Infectious Diseases, Shiga University of Medical Science, Shiga, Japan

[2]Department of Stem Cell Biology and Regenerative Medicine, Shiga University of Medical Science, Shiga, Japan

[3]Division of Molecular and Diagnostic Pathology, Shiga University of Medical Science, Shiga, Japan

[4]Division of Molecular Physiological Chemistry, Shiga University of Medical Science, Shiga, Japan

[5]Department of Urology, Kohka Public Hospital, Shiga, Japan

[6]Division of Enzyme Chemistry, Institute for Enzyme Research, The University of Tokushima, Tokushima, Japan

[7]Kitasato Institute for Life Sciences, Kitasato University, Tokyo, Japan

[8]Institute for Theoretical Medicine, Inc., Kanagawa, Japan

Abstract

Phosphorylation of pyruvate dehydrogenase by pyruvate dehydrogenase kinase 4 (PDK4) 4 inhibits its ability to induce a glycolytic shift. PDK4 expression is frequently upregulated in various cancer tissues, with its elevation being critical for the induction of the Warburg effect. PDK4 is an attractive target for cancer therapy given its effect on shifting glucose metabolism. Previous research has highlighted the necessity of identifying a potent compound to suppress PDK4 activity at the submicromolar concentrations. Here we identified natural diterpene quinones (KIS compounds) that inhibit PDK4 at low micromolar concentrations. KIS37 (cryptotanshinone) inhibited anchorage-independent growth in three-dimensional spheroid and soft agar colony formation assays of KRAS-activated human pancreatic (MIAPaCa-2 and Panc-1) and colorectal (DLD-1 and HCT116) cancer cell lines. KIS37 also suppressed KRAS protein expression in such cell lines. Furthermore, KIS37 suppressed phosphorylation of Rb protein and cyclin D1 protein expression via the PI3K-Akt–mTOR signaling pathway under nonadherent culture conditions and suppressed the expression of cancer stem cell markers CD44, EpCAM, and ALDH1A1 in MIAPaCa-2 cells. KIS37 also suppressed pancreatic cancer cell growth in both subcutaneous xenograft and orthotopic pancreatic tumor models in nude mice at 40 mg/kg (intraperitoneal dose) without any evident toxicity. Reduced ALDH1A1 expression was observed in KIS37-treated pancreatic tumors, suggesting that cancer cell stemness was also suppressed in the orthotopic tumor model. The aforementioned results indicate that KIS37 administration is a novel therapeutic strategy for targeting PDK4 in KRAS-activated intractable human pancreatic cancer.

KEYWORDS

cancer stem cell, cryptotanshinone, KRAS, pancreatic neoplasm, PDK4 inhibitor

1 | INTRODUCTION

A majority of proliferating tumor cells preferentially metabolize glucose through glycolysis, even under aerobic conditions. This phenomenon is known as the Warburg effect and is a primary metabolic hallmark of cancer cells.[1-3] Recently, the molecular mechanisms and relationships associated with cancer-related genes, including *p53*, *c-myc*, and *ras*, have been comprehensively investigated.[4,5] We had previously reported that the tumor suppressor *drs/SRPX*, which is downregulated by v-Src and activated oncogenes including *KRAS*, is involved in the shift toward glucose metabolism.[6] The loss of *drs/SRPX* contributed to the induction of the Warburg effect by upregulating lactate dehydrogenase (LDH)-B and pyruvate dehydrogenase kinase 4 (PDK4), suggesting that PDK4 and LDH-B are critical for the remodeling of glucose metabolism in malignant cancers. PDK4 is one of four PDK isoforms (PDK1–4) that control the pyruvate dehydrogenase (PDH) complex.[7] Phosphorylation of PDH by PDK inhibits its ability to induce a glycolytic shift, promoting cytoplasmic glycolysis over mitochondrial oxidative phosphorylation. Studies have revealed that PDK4 expression is frequently upregulated in various cancer tissues, with its elevation being critical for the induction of the Warburg effect.[7,8] Recently, Trinidad et al[9] reported that PDK4 knockdown by specific siRNA downregulates mutant *KRAS* expression and consequently suppresses cell growth in lung and colorectal cancer (CRC) cells, suggesting PDK4 to be an attractive target for cancer therapy. Despite reports showing the therapeutic inhibition of PDK activity by dichloroacetate (DCA),[10-12] the IC$_{50}$ value needed for PDK4 inhibition was as high as 57.8 to 500 μM,[7,13] and DCA exhibited reversible peripheral neuropathy in some clinical trials.[10,14] Although AZD7545, AZ12, and Nov3r inhibit PDK isozymes 1, 2, and 3 at the nanomolar order concentration, they have been found to stimulate PDK4 activity.[15] Thus, previous research highlights the necessity of identifying a new compound to suppress PDK4 activity at submicromolar concentrations.

Since 1980s, Nakano and Omura[16] have discovered staurosporine and related substances thereof as a protein kinase inhibitor. Although PDK is a Ser/Thr kinase, it was not inhibited by staurosporine, which had been recognized as a powerful universal kinase inhibitor. Structural analysis of the PDK4 adenosine triphosphate (ATP) binding site revealed that staurosporine was unable to attach thereto. After subsequently searching for new compounds that could inhibit PDK4 at the micromolar order from natural molecules smaller than staurosporine, we finally discovered KIS37 (cryptotanshinone) and several related compounds. Thus, this study aims to investigate the effects of KIS37 on human pancreatic and CRC cells containing mutant *KRAS*.

2 | MATERIALS AND METHODS

2.1 | Cell culture

Human pancreatic ductal adenocarcinoma (PDAC) cell lines MIAPa-Ca-2 and Panc-1; CRC cell lines DLD-1, HCT116, HT29, and WiDr; and human skin keratinocyte cell line HaCaT were obtained from the American Type Culture Collection (Manassas, VA). All cells were maintained under culture with Dulbecco's modified Eagle's medium (DMEM) supplemented with 10% fetal calf serum, penicillin (100 U/mL), and streptomycin (100 μg/mL) at 37°C in a humidified 5% CO$_2$ atmosphere. In addition, nonadherent culture was conducted by coating the dishes with poly-(2-hydroxyethyl methacrylate) reagent (poly-HEMA; Sigma-Aldrich, St Louis, MO).

2.2 | Reagents

KIS37 (cryptotanshinone) and KIS38 (tanshinone IIA) were purchased from Cosmo Bio (Tokyo, Japan), KIS116 and KIS130 from Sigma-Aldrich, KIS138 and KIS139 from Phyto Express (Columbus, OH), and sodium dichloroacetate from Wako Pure Chemical Industries, Ltd. (Osaka, Japan). AZD7545 was purchased from Cayman Chemical (Ann Arbor, MI). All reagents, except DCA, were dissolved in dimethyl sulfoxide (DMSO) to prepare 1 to 20 mM stock solutions for in vitro experiments. The final concentration of DMSO was adjusted to 0.1%. DCA was dissolved in distilled water.

2.3 | Off-chip mobility shift assay

We determined the inhibitory activities of test reagents for PDK2 and PDK4 using the off-chip mobility shift assay[13,17] by assessing E1 subunit phosphorylation of PDH in the presence of 100 μM ATP. Briefly, 5 μL of the fourfold concentration test reagent solution prepared with assay buffer (20 mM 4-(2-hydroxyethyl)-1-piperazineethanesulfonic acid [HEPES], 0.01% Triton X-100, and 2 mM dithiothreitol pH 7.5) was mixed with 5 μL of the fourfold concentration substrate (recombinant human PDH) and 10 μL of the twofold concentration human recombinant PDK/ATP–metal solution in a polypropylene 384-well plate. The mixture was then allowed to react for 5 hour at room temperature, after which 60 μL of termination buffer (QuickScout Screening Assist MSA; Carna Biosciences, Natick, MA) was added. The substrate peptide (S) and a phosphorylated peptide (P) were separated using the gel shift assay on the LabChip3000 System (Caliper Life Science, Hopkinton, MA). The inhibitory rate of each well was evaluated from the phosphorylation activity (P/[P + S]) of wells containing all reaction components (0% inhibition) and those without the enzyme (100% inhibition). The IC$_{50}$ value of each test reagent was then determined from the inhibitory rate.

2.4 | Cell proliferation assays

The soft agar assay[6] and three-dimensional (3D) spheroid formation assay[18] using 96-well V plates (PrimeSurface; Sumitomo Bakelite Co., Tokyo, Japan) were performed as described previously. To determine the number of viable cells in the 3D spheroid, the ATP present was quantified using the luminescence-based CellTiter-Glo 3D cell viability assay (Promega, Madison, WI). The viability of adherent cells was determined using CellTiter-Glo cell viability assay (Promega).

2.5 | Small interfering RNA and plasmid transfection

For the small interfering RNA (siRNA) experiment, 50 nM of Silencer Select PDK4 siRNA (s10262; Thermo Fisher Scientific, Waltham, MA) was transfected with Lipofectamine RNAiMax (Invitrogen, Carlsbad, CA) for 96 hours according to the manufacturer's protocol. A nonspecific siRNA duplex (GeneDesign, Inc, Osaka, Japan) served as the control. For plasmid transfection, pcDNA3.1 or pcDNA-myrAkt (a kind gift from Dr Masahiro Aoki, Aichi Cancer Center Research Institute) was transfected with Lipofectamine PLUS reagent (Invitrogen) according to the manufacturer's protocol.

2.6 | Immunoblotting and antibodies

A total of 5×10^5 cells were inoculated in poly-HEMA-coated 60-mm dish and cultured with KIS37 for 48 hour under nonadherent culture conditions for immunoblot analyses. Preparation of cell lysates and immunoblot analyses were carried out as described previously.[6] Mouse monoclonal antibodies for α-tubulin (DM1A) and KRAS (F234) were purchased from Sigma-Aldrich. Anti-ALDH1A rabbit monoclonal (EP1933Y), anti-LDHB rabbit polyclonal (ab75167), anti-PDH mouse monoclonal (ab110330), anti-phospho-PDH rabbit polyclonal (phospho S293, ab92696), and anti-PDK4 rabbit polyclonal (ab63157) antibodies were purchased from Abcam (Tokyo, Japan). Rabbit monoclonal antibodies for 4E-BP1 (53H11), phospho-4E-BP1 (236B4), phospho-Akt (T308, D25E6), cyclin D1 (92G2), Erk1/2 (137F5), phospho-Erk1/2 (T202/Y204, 20G11), GLUT1 (D3J3A), LDHA (C4B5), MEK1/2 (47E6), phospho-MEK1/2 (S221, 166F8), PKM2 (D78A4), S6K (49D7), PI3K (19H8), and phospho-S6K (T389, 108D2), rabbit polyclonal antibodies for Akt (#9272) and phospho-PI3K (Y458, #4288), and mouse monoclonal antibodies for CD44 (156-3C11) and EpCAM (VU1D9) were purchased from Cell Signaling Technology (Tokyo, Japan). Mouse monoclonal antibody for Rb (G3-245) was purchased from BD Biosciences (Bedford, MA).

2.7 | Quantitative reverse transcription-polymerase chain reaction analysis

Total RNA was isolated from cultured cells using Sepasol RNA I Super G (Nacalai Tesque, Kyoto, Japan). Isolated RNA was used for first-strand complementary DNA (cDNA) synthesis using SuperScript III (Invitrogen) and an oligo-dT primer for 50 minutes at 42°C. Quantitative reverse transcription-polymerase chain reaction analysis (qRT-PCR) was performed on a LightCycler 480 System using the LightCycler 480 SYBR Green I master mix (Roche Diagnostics, Tokyo, Japan) in a 20-μL reaction volume containing 1 μL template cDNA (equivalent to 100 ng total RNA) and 0.5 μM of forward and reverse primers, according to the manufacturer's protocol. Primer sequences used for qRT-PCR were as follows: *PDK4*, 5′-CCCGCTGTCCATGAAGCAGC-3′ (forward) and 5′-CCAATGTGGCTTGGGTTTCC-3′ (reverse); *Transferrin receptor* (*TFRC*), 5′-CCACCAAACAAGTTAGAGAATGC-3′ (forward) and 5′-TCAGAGCGT CGGGGATATCG-3′ (reverse). Amplification was performed as follows:

95°C for 5 minutes and 45 cycles of 95°C for 10 seconds, 55°C for 10 seconds, and 72°C for 10 seconds.

2.8 | Laboratory animals

Female 5- to 6-week-old BALB/c-nu/nu nude mice were purchased from CLEA Japan, Inc (Tokyo, Japan) and housed in a specific pathogen-free room with controlled temperature (20°C-22°C) and humidity (50%-60%) and a preset light-dark cycle (12:12 hours). All mice were allowed ad libitum access to food (CE-2; CLEA Japan, Inc) and water. The use of animals in the experimental protocols was reviewed and approved by the Management Committee of the Research Center for Animal Life Science at Shiga University of Medical Science (Shiga, Japan).

2.9 | Subcutaneous xenograft tumorigenicity assay in nude mice

The right dorsal flank of each nude 6-week-old mouse was subcutaneously injected with 5×10^6 MIAPaCa-2 cells. Two weeks after the instillation, mice were intraperitoneally administered 40 mg/kg of KIS37, suspended in 8% DMSO and 2% Solutol (Kolliphor; Sigma-Aldrich), or a vehicle (8% DMSO and 2% Solutol) once daily for 2 weeks. Mice were then killed 8 weeks after the last administration, and tumors that developed on the back of the mice were resected and fixed with 10% buffered formalin.

2.10 | Orthotopic pancreatic tumorigenicity assay in nude mice

Ten 5-week-old mice were anesthetized through isoflurane inhalation followed by an intraperitoneal injection of pentobarbital (50 mg/kg). The abdominal cavity was opened using a 1.5-cm wide longitudinal laparotomy pointing slightly to the left. Then, 1×10^6 MIAPaCa-2 cells in 100 μL of DMEM were gradually injected into the tail of the pancreas with a 27-gage needle. Both the operation and injection were always performed by the same person (CJK and YT, respectively). The pancreas was placed back into the abdominal cavity, which was then closed using interrupted suturing with 4-0 Nylon, and penicillin G (200 U/20 g) was injected intramuscularly to prevent the postoperative infection. Seven days after the injection, five mice were intraperitoneally administered 40 mg/kg of KIS37, suspended in 8% DMSO and 2% Solutol, once daily for 2 weeks. Control mice were daily administered a vehicle (8% DMSO and 2% Solutol). Finally, mice were killed a day after the last administration, after which the pancreas, liver, heart, lungs, and kidneys were resected and fixed with 10% buffered formalin.

2.11 | Histopathological analyses

Serial 3-μm sections of formalin-fixed, paraffin-embedded tissues were evaluated histologically with hematoxylin and eosin staining. For immunochemical analyses, dewaxed sections were assessed using

anti-Ki67 (Novocastra; Leica Biosystems, Nussloch, Germany), anti-ALDH1A1, and anti-phospho-PDH antibodies via the streptavidin-biotin-peroxidase methods (Histofine MAX-PO[MULTI], Nichirei, Tokyo). CD44 analysis in subcutaneous tumors was performed using the immunofluorescence staining method with anti-CD44 antibody. For the quantification of pancreatic cancer derived from MIAPaCa-2 cells, dewaxed pancreatic tissue sections were assessed using anti-hEGFR antibody (MA5-16359; Thermo Fisher Scientific) via the streptavidin-biotin-peroxidase methods and scanned using Nikon Coolscan 5000 (Nikon, Tokyo, Japan). We stained at least two longitudinal pancreatic sections per mouse, calculated the area of hEGFR-positive cancer using the ImageJ software (1.51 hours; NIH, Bethesda, MD), and used the maximum value in each pancreas as the area index.

2.12 | Statistical analyses

All quantitative data are presented as mean ± standard deviations (SD). Tukey's multiple comparison test, Welch's t test, and the Wilcoxon signed-rank test were used for statistical analyses. All statistical analyses were performed using the R statistical software package, version 2.6.2 (R Foundation for Statistical Computing, Vienna, Austria) with $p < .05$ being considered statistically significant.

3 | RESULTS

3.1 | PDK4-inhibitory activities of plant diterpene quinones in vitro

This study focused on plant-based diterpene quinone compounds, that is, KIS37, 38, 116, 130, 138, and 139, as candidates for specific PDK4 inhibitors (Figure 1). First, the off-chip mobility shift assay for PDK2 and PDK4 was performed on selected compounds and a positive control compound, DCA. DCA was able to suppress both PDK2 and PDK4 at sub-millimolar IC_{50} concentrations (610 and 330 μM, respectively; Table 1). KIS37 suppressed PDK4 and PDK2 at an IC_{50} of 11 and more than 30 μM, respectively. KIS38, 130, and 139 did not inhibit PDK4 (>30 μM). Furthermore, KIS116 and 138 suppressed both PDK2 and PDK4 at an IC_{50} of 5 to 13 μM. On the basis of these results, KIS37 was selected as the most potent and specific PDK4 inhibitor among the compounds tested.

3.2 | Effect of KIS37 on colorectal and pancreatic cancer cell lines in vitro

To assess the antioncogenic activity of KIS37, we investigated its suppressive effects on the anchorage-independent growth of four human cancer cell lines with the KRAS mutation, two CRC cell lines (DLD-1 and HCT116), and two PDAC cell lines (MIAPaCa-2 and Panc-1). KIS37 significantly suppressed colony formation of these cancer cell lines in soft agar at 1 to 10 μM (Figure 2A), although the intensity of suppression somehow varied in each cell line. In addition, the antioncogenic effect of KIS37 was assessed in 3D spheroid formation models. Accordingly, KIS37 treatment (3–10 μM) dose-dependently decreased the ATP
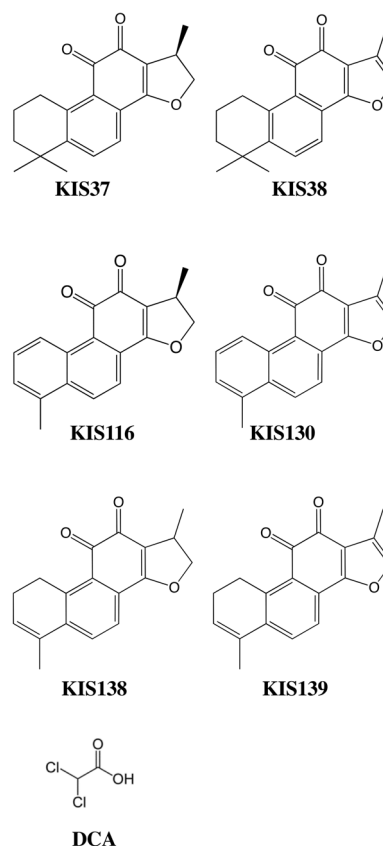

FIGURE 1 Chemical structures of KIS37 and related diterpene quinone compounds

concentration in the cell lines, which is closely correlated with the number of viable cancer cells in the spheroids (Figure 2B). Furthermore, we assessed whether apoptosis was involved in the antioncogenic effect of KIS37. The activity of caspases-3/7, a biochemical hallmark of apoptosis, was measured in the same 96-well system as the 3D spheroid assay (Figure S1). Caspases-3/7 activities were dose-dependently decreased by KIS37 treatment (Figure S1A) similar to the ATP activity (Figure 2B). Caspase-3 cleavage in KIS37-treated MIAPaCa-2 cells was not observed during immunoblot analysis (Figure S1B). These results indicated that KIS37 did not induce apoptosis under these experimental culture conditions. KIS37 treatment also inhibited the growth of these cancer cell lines under adherent culture conditions (Figure 2C). The

TABLE 1 IC_{50}s of KIS compounds for PDK2 and PDK4

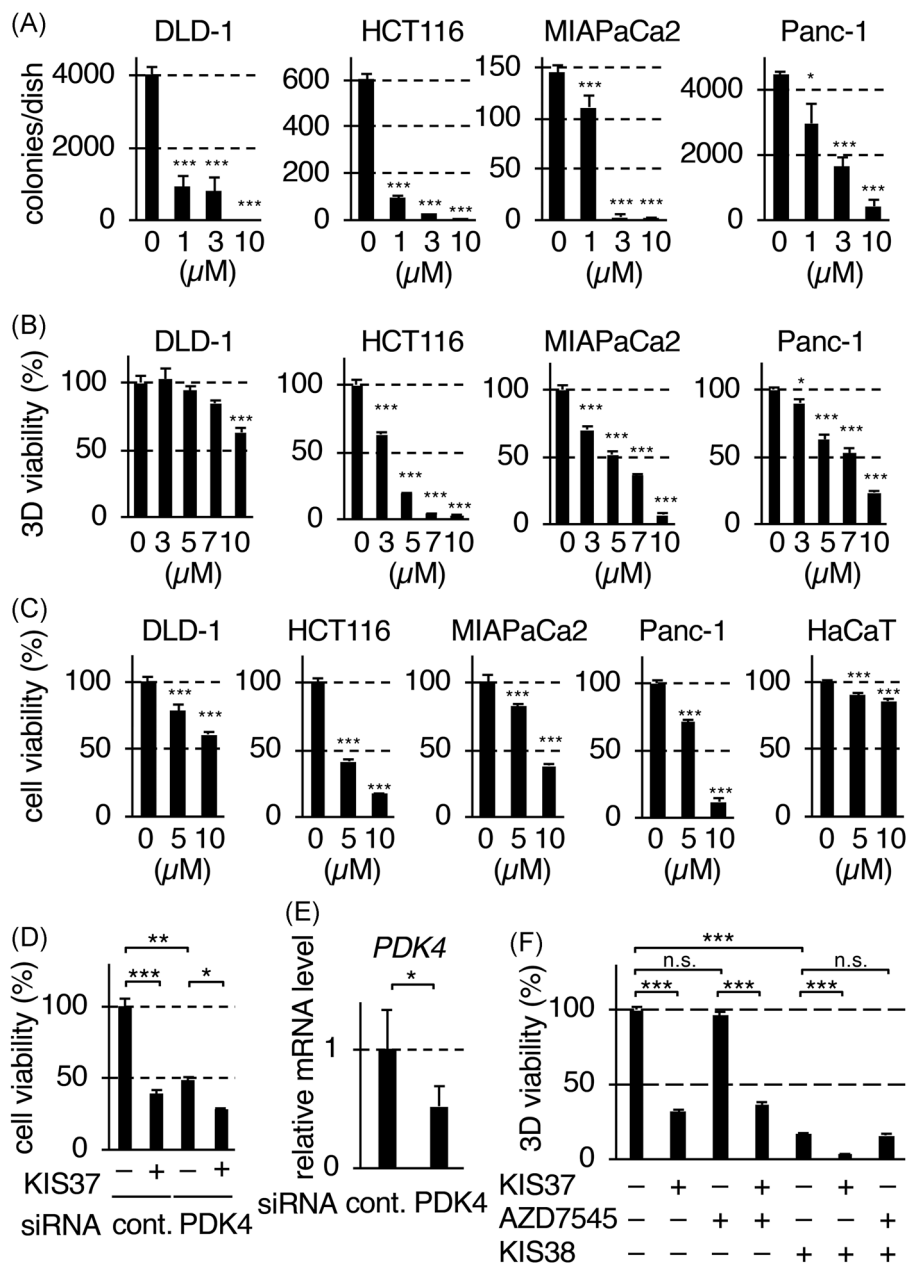| Compounds	Molecular weight	IC_{50} (μM)	
		PDK4	PDK2
KIS37 (Cryptotanshinone)	296.4	11	>30
KIS38 (Tanshinone IIA)	294.3	>30	>30
KIS116 (Dihydro tanshinone I)	278.3	5	10
KIS130 (Tanshinone I)	276.3	>30	>30
KIS138 (Tetrahydro tanshinone I)	280.3	5	13
KIS139 (1,2-Dihydro tanshinone I)	278.3	>30	>30
DCA (Dichloroacetic acid)	150.9	330	610

FIGURE 2 Effects of KIS37 on human pancreatic ductal adenocarcinoma and colorectal cancer cell lines in vitro. Error bars represent mean ± SD; *P < .05, **P < .01, and ***P < .001 using Tukey's test compared to no treatment, respectively. A, soft agar colony formations of cell lines treated with KIS37 for 3 weeks. A total of 5×10^4 cells were plated on a 60-mm dish containing 0.4% Noble agar. Each assay was tested in duplicate dishes over three independent experiments. B, 3D spheroid viability of cell lines treated with KIS37. A total of 1×10^3 cells were cultured in a 96-well V plate with KIS37 for 72 hours in triplicate. ATP content was assessed using CellTiter-Glo 3D assays. C, Cell viability under adherent culture conditions with KIS37. A total of 1×10^3 cells were cultured in a 96-well flat bottom plate for 24 hours and then treated with KIS37 for 24 hours in triplicate. ATP content was assessed using CellTiter-Glo assays. D, KIS37 effect on the viability of PDK4 siRNA-transfected MIAPaCa-2 cells under adherent culture conditions. Control or PDK4 siRNA-transfected cells were cultured for 72 hours and then treated with KIS37 for 24 hours. ATP content was assessed using CellTiter-Glo assays. Each assay was tested in duplicated dishes over two independent experiments. E, qRT-PCR analyses for *PDK4* mRNA in control or PDK4 siRNA-transfected MIAPaCa-2 cells. Data are the average of three replicates and normalized to *TFRC*. F, effects of KIS37, AZD7545, and KIS38 (5 μM each, 72 hours) on 3D spheroid viability in MIAPaCa-2 cells. A total of 1×10^3 cells were cultured in a 96-well V plate with these reagents for 72 hours in triplicate. ATP content was assessed using CellTiter-Glo 3D assays. ATP, adenosine triphosphate; mRNA, messenger RNA; ns, not significant; qRT-PCR, quantitative reverse transcription-polymerase chain reaction; siRNA, small interfering RNA; 3D, three dimensional

inhibitory effect was weak in noncancerous HaCaT cells. These results suggest that KIS37 showed cancer-specific growth inhibition without apoptosis.

To confirm whether the growth suppressive effect of KIS37 was mainly caused by PDK4 inhibition, we investigated the effect of PDK4-specific siRNA on KIS37-mediated growth suppression of

MIAPaCa-2 cells under adherent culture conditions (Figure 2D). Accordingly, siRNA for PDK4 significantly suppressed MIAPaCa-2 cell growth, indicating that PDK4 is critical for the inhibition of MIAPaCa-2 cell growth. In cells transfected with control siRNA, KIS37 (5 μM) markedly suppressed cell growth (61% inhibition). On the contrary, KIS37 in cells transfected with PDK4 siRNA had significantly lower growth suppressive effects than those transfected with control siRNA, although KIS37 moderately suppressed growth (41% inhibition) in PDK4 siRNA-transfected cells. The effect of PDK4 siRNA on the suppression of PDK4 messenger RNA (mRNA) expression was confirmed using qRT-PCR (Figure 2E). These results indicate that KIS37 mainly targeted PDK4 for the suppression of MIAPaCa-2 cell growth. To further confirm whether the effect of KIS37 on the suppression of 3D spheroid formation was specific to PDK4 inhibition, we investigated the effect of another PDK inhibitor, AZD7545, which has been shown to inhibit PDK1-3 but not PDK4,[15] in MIAPaCa-2 cells (Figure 2F). AZD7545 treatment (5 μM) did not inhibit 3D spheroid formation in MIAPaCa-2 cells, although KIS37 markedly inhibited it under the same concentration. The combination of AZD7545 and KIS37, as well as KIS37 treatment alone, also significantly inhibited 3D spheroid formation. KIS38 treatment (tanshinone IIA, 5 μM), which did not inhibit PDKs (Table 1) but was reported to inhibit other target molecules such as AP-1,[19,20] also significantly inhibited 3D spheroid formation in MIAPaCa-2 cells, with the combination of KIS37 and KIS38 synergistically also inhibiting the same. However, the combination of KIS38 and AZD7545 did not show any synergistic effect. These results indicate that suppression of 3D spheroid formation by KIS37 was also due to PDK4 inhibition.

3.3 | Changes in cancer-related proteins after KIS37 treatment

To elucidate the mechanism by which KIS37 exerts its antioncogenic action, we focused on MIAPaCa-2 cells. Initially, the effect of KIS37 on PDK4 activity was evaluated by monitoring the phosphorylation of PDH, the target protein of this kinase, in the mentioned cell line. Notably, 5 to 10 μM of KIS37 effectively suppressed PDH phosphorylation at serine 293, a hallmark of PDH activity,[21] in a dose-dependent manner under nonadherent culture conditions (Figure 3A). The expression levels of PDH protein, and α-tubulin, an internal control protein, remained unaffected by KIS37 treatment. This effect was also confirmed in the cells treated with KIS37 under adherent culture conditions (Figure S2). We then assessed changes in the expression of other glycolysis pathway regulatory proteins in MIAPaCa-2 cells (Figure 3A). The expression levels of LDH-A and LDH-B, which metabolize pyruvate into lactate, PKM2, which catalyzes phosphoenolpyruvate into pyruvate, and GLUT1, which uptakes glucose into the cell, were not affected by KIS37 treatment. These results suggest that KIS37 specifically inhibited PDK4 activity to suppress PDH phosphorylation among glycolytic regulatory proteins in MIAPaCa-2 cells.

To investigate the molecular mechanism of growth suppression by KIS37 under nonadherent culture conditions, we focused on the activated KRAS protein given that PDK4 knockdown by specific siRNA downregulated mutant KRAS expression to suppress cell growth in lung and CRC cells.[9] KRAS protein expression in MIAPaCa-2 cells was significantly downregulated following KIS37 treatment (Figure 3B), as well as under adherent culture conditions (Figure S2). In addition, effect of KIS37 on *KRAS* mRNA expression was assessed using qRT-PCR in MIAPaCa-2 cells (Figure S3). Accordingly, *KRAS* mRNA levels did not decrease after KIS37 treatment, indicating that KRAS protein suppression by KIS37 occurred at the posttranscriptional level. We then confirmed the suppressive effect of KIS37 treatment on PDH phosphorylation and KRAS protein expression in other cell lines (Figure S4). The effects observed were similarly in cells containing mutant *KRAS* (Panc-1, DLD-1, and HCT116) but were less potent in those containing wild-type *KRAS* (HT29 and WiDr). The suppressive effect of KIS37 on 3D spheroid formation was also compared between CRC cell lines containing mutant *KRAS* and those containing wild-type *KRAS*. As shown in Figure 3C, KIS37 had a significantly lower suppressive effect in HT29 and WiDr than in DLD-1 and HCT116, suggesting that the growth inhibitory effect of KIS37 was more potent in mutant *KRAS*-containing cancer cells. The expression of cyclin D1 and phosphorylation of RB (upper band), regulators of the G1-S cell cycle transition, were also reduced after KIS37 treatment under nonadherent culture conditions, consistent with the results of anchorage-independent growth and 3D spheroid assays (Figure 3B). We also assessed alterations in the expression of cancer stem cell markers CD44, EpCAM, and ALDH1A1 (Figure 3B). Accordingly, KIS37 suppressed the expression of these cancer stem cell marker proteins in MIAPaCa2 cells. These results suggest that KIS37 can suppress the cancer stem cell phenotype in MIAPaCa-2 cells.

Furthermore, changes in phosphorylation-dependent signaling pathways downstream of KRAS, such as MEK–Erk and PI3K-Akt-mTOR, were evaluated in MIAPaCa-2 cells. The present study found that KIS37 treatment did not alter MEK phosphorylation but increased Erk phosphorylation (Figure 3D). However, KIS37 treatment decreased PI3K and Akt phosphorylation. Moreover, KIS37 treatment suppressed the phosphorylation of S6K and 4EBP, targets of mTOR kinase. A similar effect was also observed in other cell lines containing mutant *KRAS* (Figure S5). To further confirm whether PI3K-Akt pathway suppression was involved in KIS37 activity, we introduced a constitutively active myristoylated Akt (myr-Akt) into MIAPaCa-2 cells (Figure 3E). The growth suppressive effects of KIS37 were significantly lower in myr-Akt-expressing cells than in those transfected with vector alone (Figure 3F). These results indicate that the PI3K-Akt pathway is critical for 3D spheroid formation resulting from KRAS protein suppression in MIAPaCa-2 cells. Overall, these results reveal that KIS37 induces KRAS downregulation resulting in the suppression of the PI3K-Akt-mTOR signaling pathway and
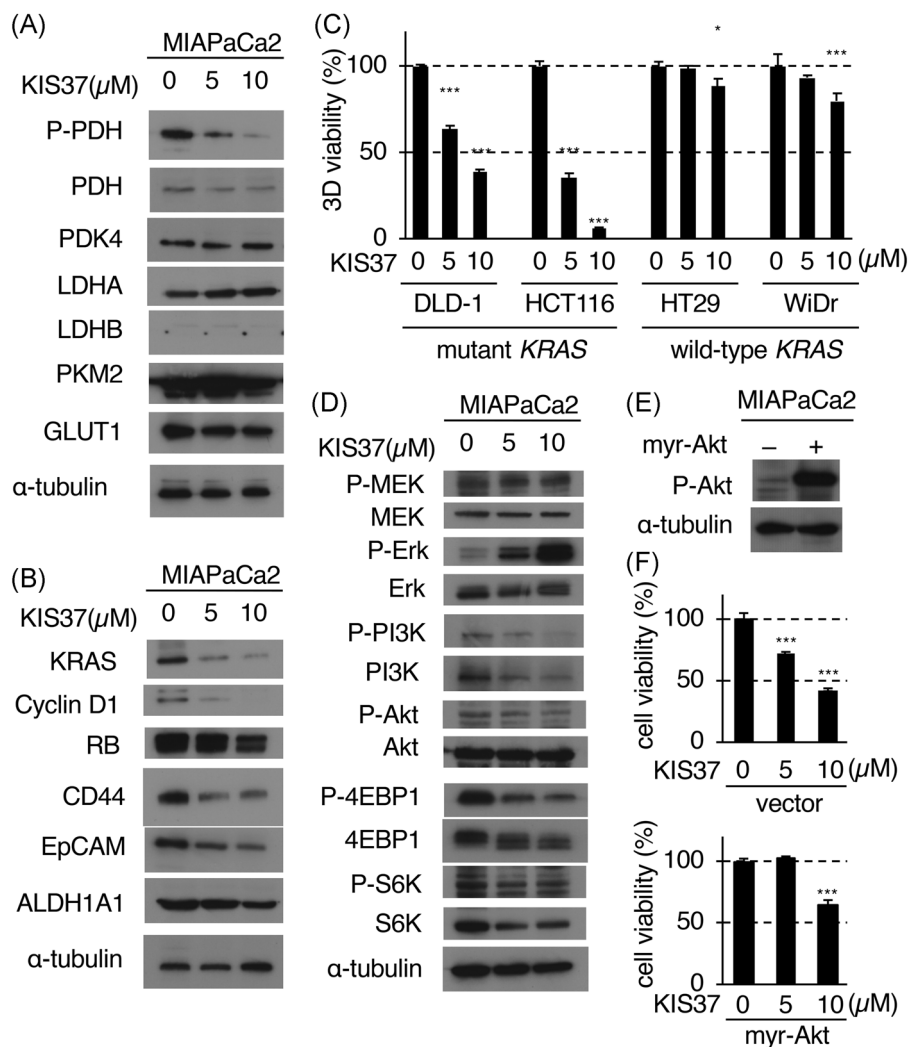
FIGURE 3 Changes in cancer-related proteins after KIS37 treatment. A, Immunoblot for proteins regulating glycolysis in nonadherent MIAPaCa-2 cells treated with KIS37 (48 hours). α-Tubulin was used as an internal control. B, Immunoblot for proteins regulating cancer cell proliferation and stemness in nonadherent MIAPaCa-2 cells treated with KIS37 (48 hours). α-Tubulin was used as an internal control. C, Suppressive effects of KIS37 on three-dimensional (3D) spheroid formation in colorectal cancer cell lines containing mutant *KRAS* (DLD-1 and HCT116) and wild-type *KRAS* (HT29 and WiDr). Adenosine triphosphate (ATP) content was assessed using CellTiter-Glo 3D assays. *$P < .05$ and ***$P < .001$ using Tukey's test compared to no treatment, respectively. D, immunoblot for Erk-MEK and PI3K-mTOR pathway proteins in nonadherent MIAPaCa-2 cells treated with KIS37 (48 hours). α-Tubulin was used as an internal control. E, Immunoblot for Akt phosphorylation in the vector (−)—or myr-Akt (+)—transfected MIAPaCa-2 cells 48 hours after transfection. α-Tubulin was used as an internal control. F, Suppressive effects of KIS37 on cell viability under adherent culture conditions of vector- or myr-Akt-transfected MIAPaCa-2 cells. Approximately 48 hours after transfection, cells were treated with KIS37 for 24 hours in triplicate. ATP content was assessed using CellTiter-Glo assays. *$P < .05$ and ***$P < .001$ using Tukey's test, respectively. ns, not significant

cell cycle progression under nonadherent culture conditions in MIAPaCa-2 cells.

3.4 | Antioncogenic effect of KIS37 in an in vivo xenograft tumorigenesis model

To determine whether KIS37 can suppress *KRAS*-mutated human pancreatic cancer cell growth in vivo, the effect of KIS37 administration was assessed in MIAPaCa-2 cells using the subcutaneous cancer cell xenograft model in nude mice. Two weeks after subcutaneous instillation of MIAPaCa-2 cells, KIS37 was administered (40 mg/kg, ip)

once daily for 2 weeks when the tumors were palpable. Although palpable tumors disappeared in two of the five KIS37-treated mice, observation for any growth or recurrence of tumors continued throughout the following 8 weeks given that tumors in each group varied in size after administration. No recurrence was observed in two of the five KIS37-treated mice whose tumors had disappeared, while KIS37-treated mice (0.026 ± 0.05 g) had significantly lesser tumor growth compared to control mice (0.68 ± 0.7 g; Figure 4A-C). Histopathological analyses revealed that cancer cells in control mice were larger and had a diffused nucleus with a higher nucleus/cytoplasm ratio (Figure 4D) compared to those in KIS37-treated mice (Figure 4E),
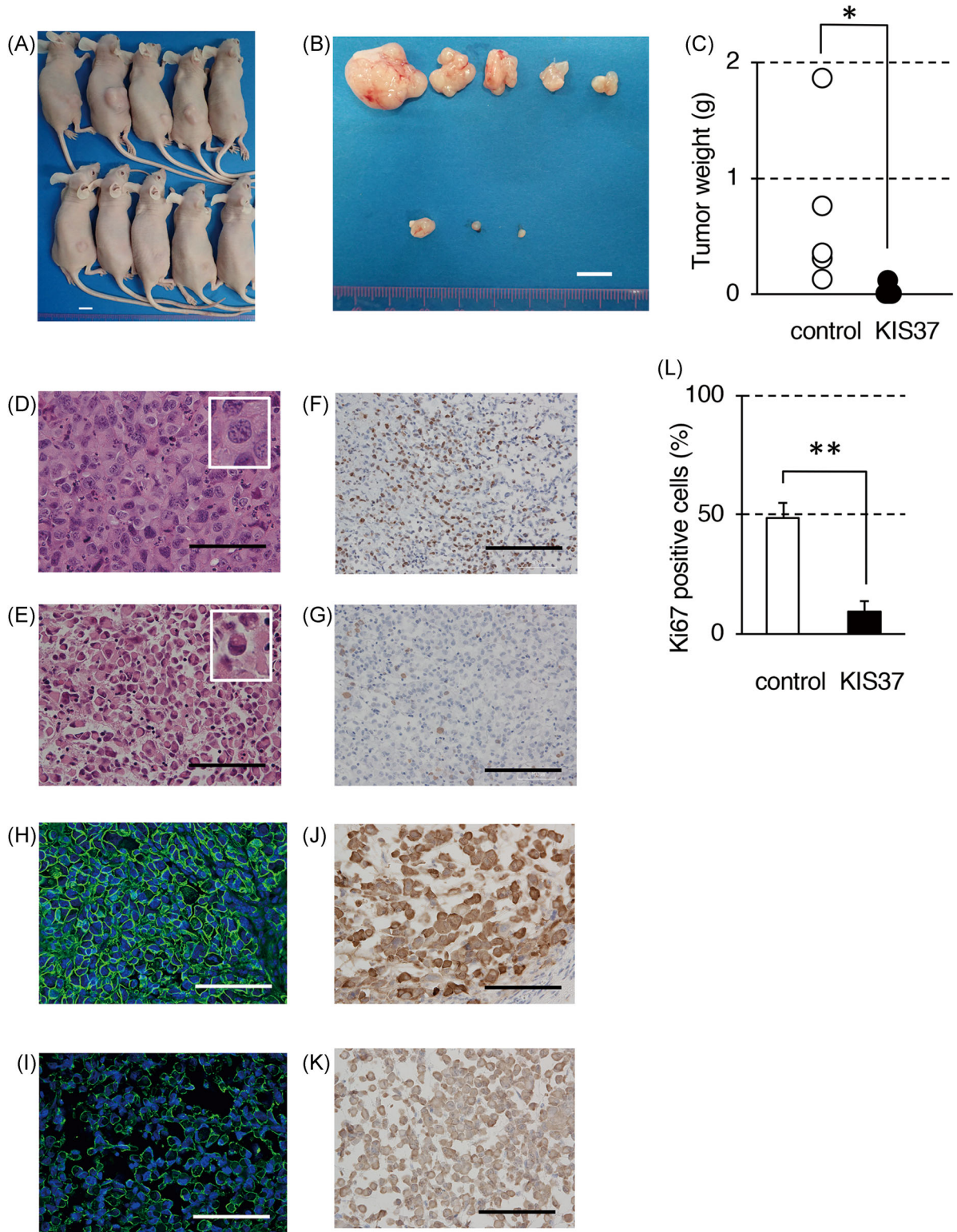
FIGURE 4 Effects of KIS37 on subcutaneous tumor growth of MIAPaCa-2 cells in nude mice. A and B, Representative tumor samples from control (top) and KIS37-injected (bottom) mice. Scale bar = 1 cm. C, Effect of KIS37 on the tumor growth. *P < .05 using the Wilcoxon test. D-K, Histopathological analyses of tumor tissues from control (D, F, H, and J) and KIS37-injected (E, G, I, and K) mice. D and E, Hematoxylin and eosin staining. F and G, Immunostaining for Ki67. H and I, Immunofluorostaining for CD44. J and K, Immunostaining for ALDH1A1. Scale bar = 100 μm. Magnification, ×400. L, Effect of KIS37 on the percentage of Ki67-positive cells. **P < .01 using t test [Color figure can be viewed at wileyonlinelibrary.com]

indicating the morphological characteristics of anaplastic malignant cancer cells. In contrast, tumor cells of KIS37-treated mice exhibited signet ring-like cellular morphology, which exhibited mucin production. In addition, KIS37-treated tumors had a significantly lower percentage of Ki67-positive cells (Figure 4F, 4G, and 4L), a marker of cell proliferation, compared to control tumors, while the number of TUNEL-positive cells (Figure S6) was similar between control and KIS37-treated tumors, suggesting that KIS37 did not induce apoptosis under these experimental conditions. The expression of CD44 (Figure 4H and 4I) and ALDH1A1 (Figure 4J and 4K), cancer stem cell markers in pancreatic cancer cells, were suppressed in KIS37-treated tumor cells. These results suggest that KIS37 can suppress in vivo tumor formation in subcutaneous xenograft models by inhibiting the growth of anaplastic cancer cells and/or cancer cells with stem-like characteristics.

3.5 | Antioncogenic effect of KIS37 in an in vivo orthotopic pancreatic tumorigenesis model

To further investigate the antioncogenic effect of KIS37 in vivo, we used the orthotopic pancreatic tumor model, which more closely mimics pancreatic tumor formation. MIAPaCa-2 cells were injected into the pancreas of nude mice, and after 1 week, KIS37 was repeatedly administered (40 mg/kg, ip) once daily for 2 weeks. Three weeks after the injection, MIAPaCa-2 cells formed a pancreatic cancer-like tumor (Figure 5A-C). Tumors derived from injected MIAPaCa-2 cells were distinguished from normal pancreatic tissues using anti-hEGFR staining (Figure 5D and 5E). Two weeks after intraperitoneal administration of 40 mg/kg KIS37, tumor formation was significantly suppressed in the pancreatic orthotopic cancer model (Figure 5F). Histopathological analyses revealed that tumor morphology in control mice was similar to that in KIS37-treated mice (Figure 5G and 5H). Tumors from KIS37-treated mice had significantly lower Ki67 expression compared to those from control mice (Figure 5I, 5J, and 5O). ALDH1A1 expression was inhibited in KIS37-treated tumors (Figure 5K and 5L). We also confirmed that KIS37-treated tumors had a greater number of intensively phosphorylated PDH-positive cells than control tumors (Figure 5M, 5N, and 5P). No abnormal behavior, body weight differences, or histopathological changes in the liver, heart, lung, and kidney were observed in both the control and KIS37-treated groups (Figure S7). Furthermore, these results confirmed the ability of KIS37 to suppress in vivo pancreatic tumor formation via PDK4 inhibition in the orthotopic mouse model.

4 | DISCUSSION

This study demonstrated the potent inhibitory activity of KIS37 against PDK4. Accordingly, KIS37 effectively inhibited PDK4 activity at low concentrations (micromolar order) to suppress in vitro phenotypes of human pancreatic and CRC cell lines. In addition, KIS37 treatment induced posttranscriptional KRAS protein downregulation in these cell lines. Trinidad et al[9] had been the first to demonstrate a correlation between PDK4 inactivation and KRAS protein downregulation using

PDK4 siRNA in human lung and CRC cells, with PDK4 siRNA suppressing cell growth in the aforementioned cancer cells. In their study, the depletion of other PDK isoforms (PDK1-3) did not suppress cancer cell growth.[9] In our study, the KIS37-induced inactivation of PDK4 suppressed PDH phosphorylation, as well as 3D spheroid formation, anchorage-independent growth, and cell growth, in human pancreatic and CRC cell lines. In MIAPaCa-2 cells, PDK4 siRNA also suppressed cell growth (Figure 2D and 2E). Inhibitor experiments in Figure 2F showed that AZD7545, an inhibitor of PDK1-3, did not suppress cell growth in MIAPaCa-2 cells, although KIS37 significantly suppressed cell growth. These results indicate that specific inhibition of PDK4 by KIS37 contributed to cell growth suppression. siRNA experiments of Figure 2D showed that KIS37 had weaker growth suppression in PDK4 siRNA-transfected cells than in control siRNA-transfected cells. Both siRNA and inhibitor experiments support the conclusion that the growth suppression by KIS37 was mainly caused by PDK4 inactivation. However, we cannot completely deny the possibility that another KIS37 target may have additionally contributed to its growth suppressive effects. Nonetheless, the strength of our strategy lies in the use of small molecules rather than specific siRNA to downregulate mutant KRAS protein expression. In the present study, KIS37 treatment also suppressed cyclin D1 protein expression under nonadherent culture conditions. In addition, we confirmed a decreased in mTOR kinase activities by monitoring KIS37 treatment-mediated phosphorylation of its target proteins, S6K and 4E-BP1. Reportedly, the mTOR pathway is downstream of the KRAS and PI3K-Akt pathway, while cyclin D1 translation is regulated downstream of 4E-BP1,[22,23] suggesting that KRAS expression downregulation suppresses cyclin D1 expression through the PI3K-Akt-mTOR pathway. Our results also showed the causal relationship between the growth suppressive effects of KIS37 and the Akt signal pathway by over-expression of constitutively active Akt. Exogeneous activation of Akt significantly inhibited cell growth suppression by KIS37.

In addition, KIS37 suppressed the expression of cancer stem cell marker proteins CD44, EpCAM, and ALDH1A1 in MIAPaCa-2 cells, implying the inhibitory effect of KIS37 on the growth of cancer stem cells. In fact, KIS37 inhibited the representative phenotypes of cancer stem cells, 3D spheroid formation, and in vivo xenograft tumor growth in MIAPaCa-2 cells. Moreover, pathological analyses of xenograft tumors revealed that differentiation was induced by KIS37 treatment (Figure 5D and 5E). The decrease in CD44 and ALDH1A1 in KIS37-treated tumors also corroborates this conclusion. Recent research has demonstrated that cancer stem cells undergo metabolic alterations, including high glycolytic activity and low mitochondrial respiration.[24] Some studies have reported that KRAS mutation alters cell metabolism and induces cancer cell stemness in various human cancer cells.[25,26] The present study suggests that cell metabolism alterations caused by the inhibition of PDK4 activity results in PDH activation, which suppresses cancer cell stemness in pancreatic cancer cells expressing mutant KRAS. The growth inhibitory effects of KIS37 was more potent in pancreatic and CRC cell lines containing mutant KRAS than in cell lines containing wild-type KRAS (Figure 3D), suggesting that KIS37 toxicity may be lower in normal cells containing wild-type KRAS protein than in cancer cells containing mutant KRAS protein.
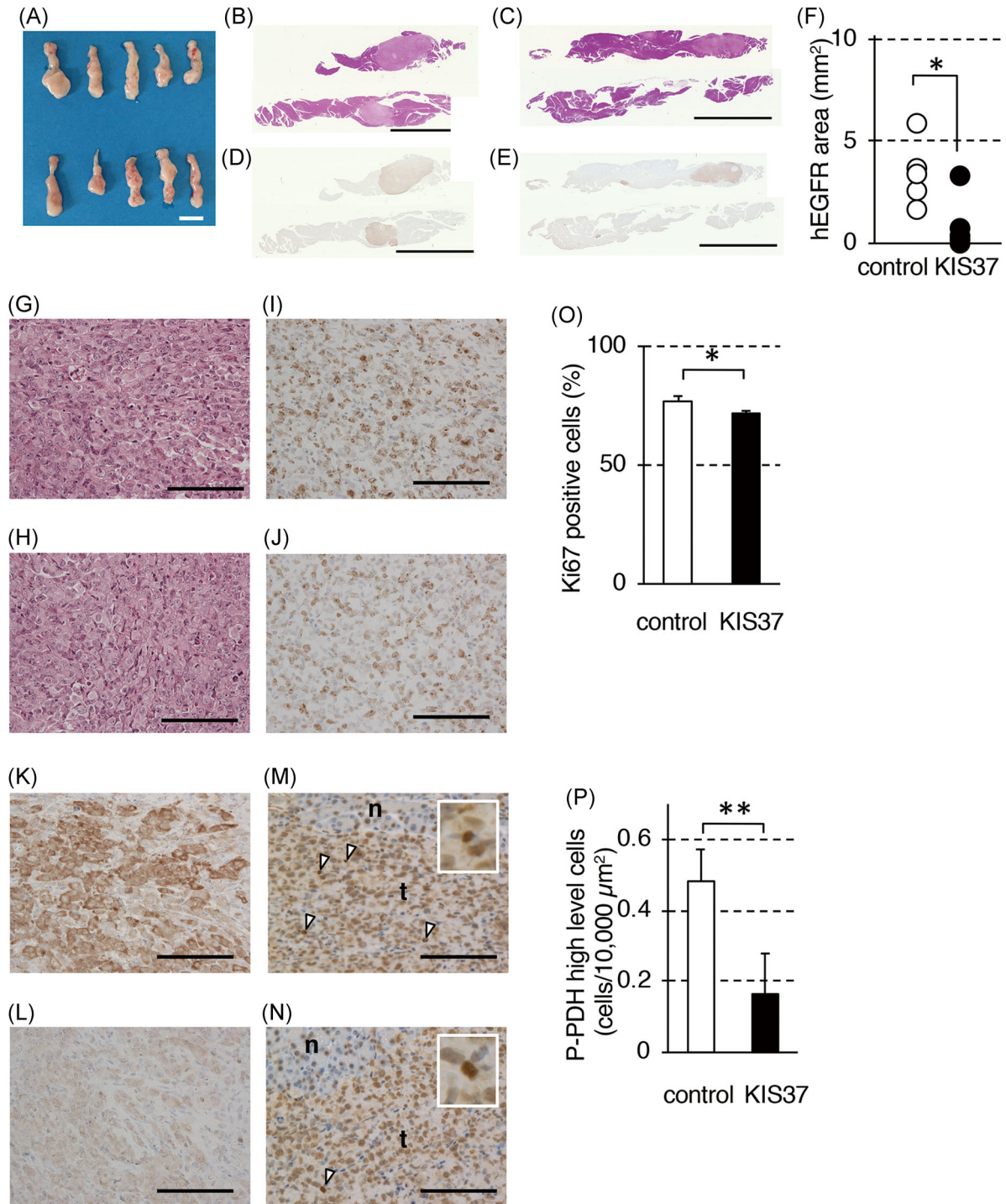
FIGURE 5 Effects of KIS37 on orthotopic pancreatic tumor growth of MIAPaCa-2 cells in nude mice. A, A representative photograph of the pancreas from control (top) and KIS37-injected (bottom) mice. Scale bar = 1 cm. B-E, Low magnification histopathological sections of the pancreas from control (B and D) and KIS37-injected (C and E) mice. Pancreas with maximum (top) and minimum (bottom) tumor sizes within each group are presented. Each bar = 5 mm. B and C, Hematoxylin and eosin (HE) staining. D and E, Immunostaining for human epidermal growth factor receptor (hEGFR). F, The indexes of the tumor area expressing hEGFR of control and KIS37-injected mice. *$P < .05$ by the Wilcoxon test. G-N, Histopathological analyses of the pancreatic tumors from control (G, I, K, and M) and KIS37 (H, J, L, and N)-injected mice. Each bar = 100 µm. Magnification, ×400. G and H, Hematoxylin and eosin staining. I and J, Immunostaining for Ki67. K and L, Immunostaining for ALDH1A1. M and N, Immunostaining for phosphorylated PDH (P-PDH). Tumor (t) and nontumor (n) areas are shown. Arrowheads show cells expressing high levels of P-PDH. O and P, Proportions of Ki67-positive (O) and high P-PDH expression (P) cells in the tumor of control and KIS37-injected mice. Scale bars = mean ± SD; *$P < .05$ and **$P < .001$ using t test, respectively [Color figure can be viewed at wileyonlinelibrary.com]

KIS37 (cryptotanshinone) and related compounds can be obtained from *Salvia miltiorrhiza* Bunge (*danshen*), a traditional Chinese herb used for the treatment of various diseases.[27] KIS37 possesses several pharmacological activities, including antidiabetic, antiobesity, antioxidative, antiangiogenic, and anti-inflammatory actions.[28,29] Furthermore, studies have revealed that KIS37 exerts antitumor effects on various human cancer types,[27-29] including prostate, breast, hepatocarcinoma, colorectal, lung, leukemia, ovarian, rhabdomyosarcoma, and melanoma cancer cells. Although KIS37 primarily inhibits the function of signal transducer and activator of transcription 3, other targets have also been suggested.[30] Here, we have identified PDK4 as a novel target of KIS37 and revealed KRAS expression downregulation as its downstream pathway for the suppression of cancer cell stemness in pancreatic cells.

The PDH-PDK axis has been considered a crucial therapeutic target in cancer[7,10,11] with PDK4 having an especially pivotal role for altered cell metabolism in malignant cancers.[7,9] This therapeutic strategy warrants small molecules that effectively inhibit PDK4 activity without exhibiting toxicity. Despite comprehensively investigating DCA and its derivatives for this purpose, desirable outcomes have not been obtained to date.[10-12] Our findings suggest that KIS37 could be a promising candidate compound for new-generation PDK inhibitors. Apparently, pancreatic cancer is among the most lethal cancer types,[31] exhibiting high invasiveness, rapid progression, and strong resistance to treatment.[31,32] Although gemcitabine has been the primary chemotherapeutic treatment option for pancreatic cancer, its clinical efficacy has been insufficient.[33] We have demonstrated the potent antioncogenic activity of KIS37 in an orthotopic mouse pancreatic tumor model system without evident side effects, suggesting that KIS37 could be a potential treatment option for intractable pancreatic cancer through its inactivation of mutant *KRAS*.

ACKNOWLEDGMENTS

CONFLICT OF INTERESTS

The authors declare that there are no conflict of interests.

DATA AVAILABILITY

The data that support the findings of this study are available from the corresponding author upon reasonable request.

ORCID

Hirokazu Inoue http://orcid.org/0000-0001-9800-9449

REFERENCES

1. Hanahan D, Weinberg RA. Hallmarks of cancer: the next generation. *Cell*. 2011;144:646-674.
2. Hsu PP, Sabatini DM. Cancer cell metabolism: Warburg and beyond. *Cell*. 2008;134:703-707.
3. Vander Heiden MG, Cantley LC, Thompson CB. Understanding the Warburg effect: the metabolic requirements of cell proliferation. *Science*. 2009;324:1029-1033.
4. Dang CV. Links between metabolism and cancer. *Genes Dev*. 2012;26:877-890.
5. Pavlova NN, Thompson CB. The emerging hallmarks of cancer metabolism. *Cell Metab*. 2016;23:27-47.
6. Tambe Y, Hasebe M, Kim CJ, Yamamoto A, Inoue H. The drs tumor suppressor regulates glucose metabolism via lactate dehydrogenase-B. *Mol Carcinog*. 2016;55:52-63.
7. Saunier E, Benelli C, Bortoli S. The pyruvate dehydrogenase complex in cancer: an old metabolic gatekeeper regulated by new pathways and pharmacological agents. *Int J Cancer*. 2016;138:809-817.
8. Leclerc D, Pham DN, Lévesque N, et al. Oncogenic role of PDK4 in human colon cancer cells. *Br J Cancer*. 2017;116:930-936.
9. Trinidad AG, Whalley N, Rowlinson R, et al. Pyruvate dehydrogenase kinase 4 exhibits a novel role in the activation of mutant KRAS, regulating cell growth in lung and colorectal tumour cells. *Oncogene*. 2017;36:6164-6176.
10. Stacpoole PW. Therapeutic targeting of the pyruvate dehydrogenase complex/pyruvate dehydrogenase kinase (PDC/PDK) axis in cancer. *J Natl Cancer Inst*. 2017;109. https://doi.org/10.1093/jnci/djx071
11. Sutendra G, Michelakis ED. Pyruvate dehydrogenase kinase as a novel therapeutic target in oncology. *Front Oncol*. 2013;3:38.
12. Kankotia S, Stacpoole PW. Dichloroacetate and cancer: new home for an orphan drug? *Biochim Biophys Acta*. 2014;1846:617-629.
13. Yamane K, Indalao IL, Chida J, Yamamoto Y, Hanawa M, Kido H. Diisopropylamine dichloroacetate, a novel pyruvate dehydrogenase kinase 4 inhibitor, as a potential therapeutic agent for metabolic disorders and multiorgan failure in severe influenza. *PLOS One*. 2014;9:e98032.
14. Chu QS, Sangha R, Spratlin J, et al. A phase I open-labeled, single-arm, dose-escalation, study of dichloroacetate (DCA) in patients with advanced solid tumors. *Invest New Drugs*. 2015;33:603-610.
15. Wynn RM, Kato M, Chuang JL, Tso SC, Li J, Chuang DT. Pyruvate dehydrogenase kinase-4 structures reveal a metastable open conformation fostering robust core-free basal activity. *J Biol Chem*. 2008;283:25305-25315.
16. Nakano H, Omura S. Chemical biology of natural indolocarbazole products: 30 years since the discovery of staurosporine. *J Antibiot (Tokyo)*. 2009;62:17-26.
17. Kitagawa D, Yokota K, Gouda M, et al. Activity-based kinase profiling of approved tyrosine kinase inhibitors. *Genes Cells*. 2013;18:110-122.
18. Kim CJ, Terado T, Tambe Y, et al. Anti-oncogenic activities of cyclin D1b siRNA on human bladder cancer cells via induction of apoptosis and suppression of cancer cell stemness and invasiveness. *Int J Oncol*. 2018;52:231-240.
19. Xu S, Liu P. Tanshinone II-A: new perspectives for old remedies. *Expert Opin Ther Pat*. 2013;23:149-153.
20. Park S, Song JS, Lee DK, Yang CH. Suppression of AP-1 activity by tanshinone and cancer cell growth inhibition. *Bull Korean Chem Soc*. 1999;20:925-928.
21. Zhang W, Zhang SL, Hu X, Tam KY. Targeting tumor metabolism for cancer treatment: is pyruvate dehydrogenase kinases (PDKs) a viable anticancer target? *Int J Biol Sci*. 2015;11:1390-1400.
22. Laplamte M, Sabatini DM. mTOR signaling in growth control and disease. *Cell*. 2012;149:274-293.
23. Nussinov R, Jang H, Tsai CJ, et al. Intrinsic protein disorder in oncogenic KRAS signaling. *Cell Mol Life Sci*. 2017;74:3245-3261.

24. Deshmukh A, Deshpande K, Arfuso F, Newsholme P, Dharmarajan A. Cancer stem cell metabolism: a potential target for cancer therapy. *Mol Cancer.* 2016;15:69.

25. Ying H, Kimmelman AC, Lyssiotis CA, et al. Oncogenic Kras maintains pancreatic tumors through regulation of anabolic glucose metabolism. *Cell.* 2012;149:656-670.

26. Perera RM, Bardeesy N. Pancreatic cancer metabolism: breaking it down to build it back up. *Cancer Discov.* 2015;5:1247-1261.

27. Su CY, Ming QL, Rahman K, Han T, Qin LP. *Salvia miltiorrhiza*: traditional medicinal uses, chemistry, and pharmacology. *Chin J Nat Med.* 2015;13:163-182.

28. Cai Y, Zhang W, Chen Z, Shi Z, He C, Chen M. Recent insights into the biological activities and drug delivery systems of tanshinones. *Int J Nanomedicine.* 2016;11:121-130.

29. Chen W, Lu Y, Chen G, Huang S. Molecular evidence of cryptotanshinone for treatment and prevention of human cancer. *Anticancer Agents Med Chem.* 2013;13:979-987.

30. Shin DS, Kim HN, Shin KD, et al. Cryptotanshinone inhibits constitutive signal transducer and activator of transcription 3 function through blocking the dimerization in DU145 prostate cancer cells. *Cancer Res.* 2009;69:193-202.

31. Heestand GM, Kurzrock R. Molecular landscape of pancreatic cancer: implications for current clinical trials. *Oncotarget.* 2015;6:4553-4561.

32. Cohen R, Neuzillet C, Tijeras-Raballand A, Faivre S, de Gramont A, Raymond E. Targeting cancer cell metabolism in pancreatic adenocarcinoma. *Oncotarget.* 2015;6:16832-16847.

33. Saung MT, Zheng L. Current standards of chemotherapy for pancreatic cancer. *Clin Ther.* 2017;39:2125-2134.

SUPPORTING INFORMATION

Additional supporting information may be found online in the Supporting Information section.